New ^{59}Fe Stellar Decay Rate with Implications for the ^{60}Fe Radioactivity in Massive Stars

B. Gao,[1,2,*] S. Giraud,[3] K. A. Li,[1,2,†] A. Sieverding,[4] R. G. T. Zegers,[3,5,6] X. Tang,[1,2] J. Ash,[3,6] Y. Ayyad-Limonge,[3] D. Bazin,[3,6] S. Biswas,[3] B. A. Brown,[3,5,6] J. Chen,[3] M. DeNudt,[3,6] P. Farris,[3,6] J. M. Gabler,[3] A. Gade,[3,5,6] T. Ginter,[3] M. Grinder,[3,6] A. Heger,[7] C. Hultquist,[3,6] A. M. Hill,[3,6] H. Iwasaki,[3,6] E. Kwan,[3] J. Li,[3] B. Longfellow,[3,6] C. Maher,[3,6] F. Ndayisabye,[3,6] S. Noji,[3,5] J. Pereira,[3,5] C. Qi,[8] J. Rebenstock,[3] A. Revel,[3] D. Rhodes,[3,6] A. Sanchez,[3,6] J. Schmitt,[3,5,6] C. Sumithrarachchi,[3] B. H. Sun,[9,10] and D. Weisshaar[3]

[1]*CAS Key Laboratory of High Precision Nuclear Spectroscopy, Institute of Modern Physics, Chinese Academy of Sciences, Lanzhou 73000, People's Republic of China*

[2]*School of Nuclear Science and Technology, University of Chinese Academy of Sciences, Beijing 100049, People's Republic of China*

[3]*National Superconducting Cyclotron Laboratory, Michigan State University, East Lansing, Michigan 48824, USA*

[4]*School of Physics and Astronomy, University of Minnesota, Minneapolis, Minnesota 55455, USA*

[5]*Joint Institute for Nuclear Astrophysics—Center for the Evolution of the Elements, Michigan State University, East Lansing, Michigan 48824, USA*

[6]*Department of Physics and Astronomy, Michigan State University, East Lansing, Michigan 48824, USA*

[7]*School of Physics and Astronomy, Monash University, Victoria 3800, Australia*

[8]*Department of Physics, Royal Institute of Technology, Stockholm 10691, Sweden*

[9]*School of Physics, Beihang University, Beijing 100191, China*

[10]*International Research Center for Nuclei and Particles in the Cosmos, Beijing 100191, China*

(Received 22 December 2020; revised 20 February 2021; accepted 17 March 2021; published 12 April 2021)

The discrepancy between observations from γ-ray astronomy of the ^{60}Fe/^{26}Al γ-ray flux ratio and recent calculations is an unresolved puzzle in nuclear astrophysics. The stellar β-decay rate of ^{59}Fe is one of the major nuclear uncertainties impeding us from a precise prediction. The important Gamow-Teller strengths from the low-lying states in ^{59}Fe to the ^{59}Co ground state are measured for the first time using the exclusive measurement of the ^{59}Co$(t, {}^3\mathrm{He}+\gamma)^{59}$Fe charge-exchange reaction. The new stellar decay rate of ^{59}Fe is a factor of 3.5 ± 1.1 larger than the currently adopted rate at $T = 1.2$ GK. Stellar evolution calculations show that the ^{60}Fe production yield of an 18 solar mass star is decreased significantly by 40% when using the new rate. Our result eliminates one of the major nuclear uncertainties in the predicted yield of ^{60}Fe and alleviates the existing discrepancy of the ^{60}Fe/^{26}Al ratio.

DOI: 10.1103/PhysRevLett.126.152701

Introduction.—The nucleosynthesis of the observable long-lived radioactive nuclides ^{60}Fe ($T_{1/2} = 2.26$ Myr) and ^{26}Al ($T_{1/2} = 0.717$ Myr) is an important constraint on the stellar models. Both isotopes are mainly synthesized in massive stars [1–3] with small contributions from other sites, such as asymptotic giant branch star, type Ia supernova, and electron capture supernova [4–7]. The abundances inferred from γ-ray astronomy may have important implications for rotationally induced mixing, convection theory, mass loss theory, the initial mass function for massive stars, and the distribution of metals in the Galaxy [3]. The present γ-ray observations determine the ^{60}Fe/^{26}Al γ-ray flux ratio to be 0.184 ± 0.042 based on the exponential disk grid maps [8]. However, the mean ratio may vary in the range of 0.2–0.4 by using different sky maps. Theory groups predict the γ-ray flux ratio at a large variation from 0.1–1 [1,3,9–11]. For example, earlier simulations successfully reproduced the observation [1], giving a ^{60}Fe/^{26}Al γ-ray flux ratio of 0.16 ± 0.12. However, later calculations by the same group predicted a much larger flux ratio of ^{60}Fe/^{26}Al $= 0.45$ [3] when using improved nuclear physics input and stellar models. They studied the sources of the discrepancy and concluded that the uncertain nuclear cross sections related to the creation and destruction of these unstable isotopes were the major sources. Thus, important inferences concerning stellar models will only be credible when these uncertain nuclear reaction rates have been better determined [3]. The goal of the present Letter is to pin down the stellar β-decay rate of ^{59}Fe, which is one of the most important nuclear physics uncertainties for predicting the yield of ^{60}Fe [12], and to provide a more solid basis for future astrophysical simulations.

^{60}Fe is mostly synthesised in massive stars during helium (He) shell burning ($T \sim 0.4$ GK), carbon (C) shell burning ($T \sim 1.2$ GK), and explosive carbon/neon (C/Ne) burning stages ($T \sim 2.2$ GK) [2]. The main nuclear reaction pathways are shown in Fig. 1. ^{59}Fe acts as a branching point at which the β-decay and neutron-capture processes compete in the synthesis of ^{60}Fe. Though the terrestrial β-decay rate

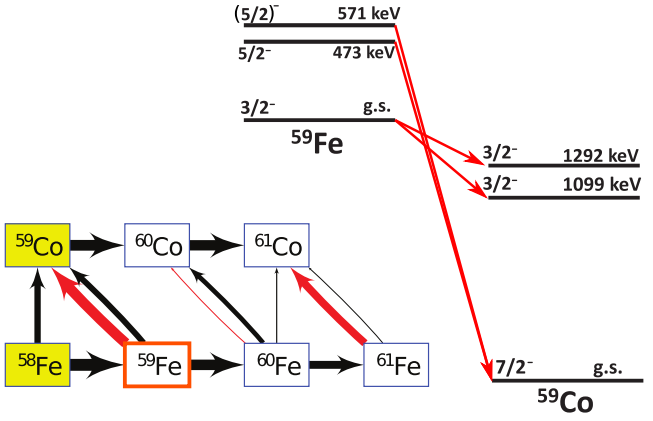

FIG. 1. Left: net reaction flow chart of ^{60}Fe nucleosynthesis in C-shell burning. The red lines are β decays and black lines are proton-(neutron-)induced reactions. Line widths represent the reaction flow in logarithmic scale. Right: Gamow-Teller transitions that are of importance for the stellar β-decay rate of ^{59}Fe during the synthesis of ^{60}Fe.

of ^{59}Fe is well determined ($T_{1/2} = 44.5$ days), its decay rate could be dramatically enhanced in stellar environments. For example, during C-shell burning, the temperature is high and the γ excitation and deexcitation processes are in equilibrium where a considerable fraction of the ^{59}Fe nuclei are in their excited states. Therefore, β decays from the excited states also contribute to the total decay rate (see Fig. 1). Because of the favorable selection rules and larger decay Q values, β decays from the excited states of ^{59}Fe are orders of magnitude faster than from the ground state. Consequently, the effective β-decay rate of ^{59}Fe in the stellar environment becomes much larger than the terrestrial one. Existing theoretical calculations, including the independent particle model calculations by Fuller-Fowler-Newman (FFN) [13], shell model calculations using modified KB3 interactions by Langanke and Martínez-Pinedo (LMP) [14], and shell model calculations [12] using more recent interactions of the GXPF family [15], predicted different β-decay rates for ^{59}Fe with large discrepancies. For example, at the typical C-shell burning temperature (1.2 GK), the calculations by FFN gave a rate 10 times larger than the currently adopted one from LMP, resulting in a variation of the ^{60}Fe yield by about a factor of 3 [12]. The stellar β-decay rate of ^{59}Fe is a major contribution to the nuclear physics related uncertainties of the ^{60}Fe production and it leads to a larger variation of the yields than the ^{59}Fe(n,γ) reaction rate. Therefore, an accurate determination of the ^{59}Fe-decay rate is required.

Direct measurement of the β-decay rate from excited states of ^{59}Fe, which decay mostly by emitting γ rays, is challenging due to the very tiny β-decay branching ratios. From theory point of view, nuclear β-decay rates depend on the decay Q value and the Gamow-Teller (GT) transition strengths [B(GT)]. Since the masses of the ^{59}Fe and ^{59}Co nuclei, and therefore the Q value, are well known, the B(GT) becomes the only missing component to calculate the β-decay rates from the ^{59}Fe excited states. Charge-exchange reactions at intermediate energies ($\gtrsim$100 MeV/u) have been proven to be a useful tool to measure [B(GT)] [16,17]. The B(GT) distribution of ^{59}Fe was previously measured via the ^{59}Co$(n,p)^{59}$Fe reaction [18]. However, the poor resolution ($\sim$0.9 MeV) did not allow an accurate determination of B(GT) value for each individual state. The measured transition strengths of the low-lying states were unresolved from the higher-lying states. In this Letter, the first exclusive measurement of ^{59}Co$(t,{}^3\mathrm{He})^{59}$Fe was performed to extract the fine structure of the transition strength to the low-lying states in ^{59}Fe. Our measurement provides the reliable B(GT) of the important transitions to accurately determine the stellar β-decay rate of ^{59}Fe.

Experiment.—The experiment was performed at the Coupled Cyclotron Facility (CCF) at the National Superconducting Cyclotron Laboratory. An ^{16}O primary beam with an intensity of 150 pnA and an energy of 150 MeV/u provided by the CCF impinged on a beryllium target with a thickness of 3525 mg/cm^2. The A1900 fragment separator [19] with a 195-mg/cm^2-thick Al degrader was used to select the tritons from other reaction products. The resulting triton beam with an intensity of $\sim 4\times 10^6$ pps and an energy of 115 MeV/u was transported to the pivot point of the S800 spectrograph [20] where a 22.25-mg/cm^2-thick ^{59}Co target was mounted. A polyethylene (CH_2) target with a thickness of 4.1 mg/cm^2 was also used to calibrate the triton beam intensity using the cross section accurately measured previously [21]. The ejectiles from reactions on the target were momentum analyzed by the S800 spectrograph and finally detected by two cathode-readout drift chambers (CRDCs) [22] and a 5-mm-thick plastic scintillator. The CRDCs measured the hit positions and track angles of the ejectiles at the focal plane, which were used to reconstruct their scattering angles and energies after the target. The plastic scintillator measured the energy loss (ΔE) and, in combination with the radio-frequency signals from the CCF, the time of flight (TOF) of the ejectiles. By using the ΔE-TOF particle identification technique, the ^{3}He particles were clearly identified from other reaction products.

The γ-ray detection system GRETINA [23,24] was placed around the reaction target to detect the deexcitation γ rays from the ^{59}Fe residual nucleus in coincidence with the ^{3}He ejectiles. The coincident measurement allows one to analyze the GT transitions with very weak strengths to the low-lying states of the residual nucleus, which are otherwise difficult to identify in the particle singles data alone [25–29].

Analysis and results.—The excitation energy of the ^{59}Fe residual nucleus was deduced by using a missing mass calculation. Double-differential cross sections were determined up to an excitation energy of 25 MeV and a

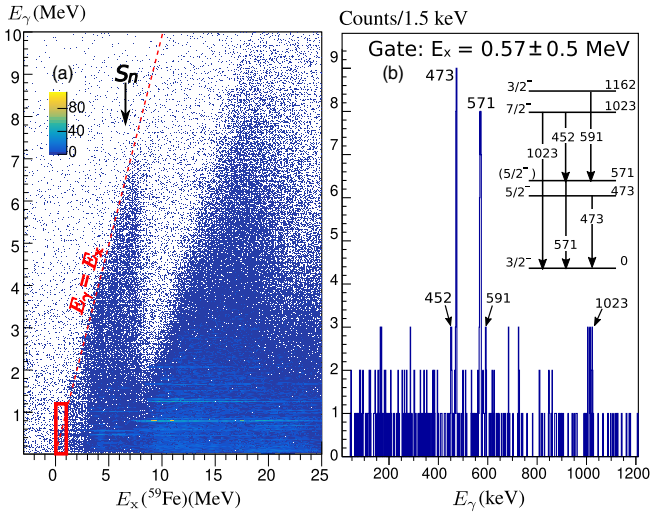

FIG. 2. (a) Two-dimensional plot of E_γ versus $E_x(^{59}\mathrm{Fe})$. The $E_\gamma = E_x$ line and the neutron separation energy ($S_n = 6.6$ MeV) are indicated. (b) Coincident γ-ray energy spectrum gated on $E_x = 0.57 \pm 0.5$ MeV. The gate is indicated by the red box in (a). The inset shows a partial level scheme of ^{59}Fe.

center-of-mass angle of 4.5° with energy and angular resolutions of 0.5 MeV and 1° (FWHM), respectively.

The present Letter mainly focuses on the transitions to the low-lying states below 1 MeV in ^{59}Fe since high-lying states have negligible contributions to the total β-decay rate during the stellar nucleosynthesis of ^{60}Fe. The coincident γ rays measured by GRETINA provide important details of those states. A two-dimensional plot of the γ-ray energy (E_γ) measured by GRETINA versus the excitation energy $E_x(^{59}\mathrm{Fe})$ deduced from the $(t, ^3\mathrm{He})$ data is shown in Fig. 2. The data points scattered in the $E_\gamma > E_x$ region are mainly from a minor contamination of ^{6}He in the triton beam, which breaks up into $^3\mathrm{He} + 3n$ at the target. Such events are not associated with excitations of ^{59}Fe and can be excluded by gating on deexcitation γ rays from ^{59}Fe. The clear drop of the γ-ray yield at $E_x \sim 8$ MeV is due to the opening of the neutron emission channel of the ^{59}Fe residual nucleus.

Among the low-lying states in ^{59}Fe, there are two known states, namely the 473- and 571-keV levels, that can be populated via GT transitions from the ground state of ^{59}Co, though the spin value of the 571-keV state is still under debate [30–33]. In this Letter, $J^\pi = 5/2^-$ is used for the 571-keV state based on the most recent experimental results [33]. Two other states with unknown spins and parities at 613- and 643-keV excitation energies also exist [32,34]. They could also potentially be GT states and contribute to the total stellar β-decay rate of ^{59}Fe. All those states mentioned above are known to decay directly to the ground state with 100% branching ratios [32,33], emitting γ rays with energies equal to their excitation energies. By setting the excitation energy $E_x(^{59}\mathrm{Fe}) < 1$ MeV, the 473- and 571-keV states were clearly seen, while the 613- and 643-keV ones were not observed in the γ-ray spectra, indicating only the former two need to be considered for calculating the stellar decay rate of ^{59}Fe.

The coincident γ-ray counts of the 473- and 571-keV states were extracted by gating on $E_x(^{59}\mathrm{Fe}) = 473/571 \pm 500$ keV where the width of the gate was chosen based on the energy resolution of the S800 for the present measurement. Figure 2 shows the gated γ-ray spectrum for the 571-keV state. The existence of the 452-, 591-, and 1023-keV peaks in the spectrum indicates that the 571-keV peak includes contributions from feedings from higher-lying states at 1023 and 1162 keV. However, their contributions can be reliably subtracted by using the counts of the 452-, 591-, and 1023-keV peaks in the gated spectrum and the corresponding branching ratios. For the 473-keV state, the only known higher-lying state that decays to it is the 1599-keV one, which is well separated from it in the excitation energy spectrum (the 1023- and 1162-keV states also decay to it but with a very small branching ratio of ~2%). Therefore, the 473-keV peak in the gated spectrum was considered free from feedings from higher-lying states.

The measured γ-ray counts can be converted to $B(\mathrm{GT})$ by using the well-established proportionality between differential cross section at zero momentum transfer $(d\sigma/d\Omega)_{q=0}$ and $B(\mathrm{GT})$,

$$\left(\frac{d\sigma}{d\Omega}\right)_{q=0} = \hat{\sigma} B(\mathrm{GT}), \tag{1}$$

where $\hat{\sigma}$ is the so-called unit cross section. Here, $B(\mathrm{GT})$ is defined such that it equals 3 for the decay of free neutrons. In the present Letter, an empirical mass-dependent formula $\hat{\sigma} = 109A^{-0.65}$ mb/sr [16] was used to obtain the $\hat{\sigma}$, where A is the mass number of the target nucleus. Though the coincident γ-ray counts represent an integrated cross section, it can be correlated to the differential cross section at zero degree $d\sigma/d\Omega(0°)$, via calculated angular distributions. The calculation was done by using the double-folding distorted-wave Born approximation (DWBA) code FOLD [35]. The single particle wave functions for t and ^{3}He were taken from variational Monte Carlo calculations [36], while those for ^{59}Fe/^{59}Co were calculated by using a Woods-Saxon potential. One-body transition densities were obtained from shell model calculations using the GXPF1a interaction [37] in the full pf shell model space. The optical model potential parameters from the $^{58}\mathrm{Ni} + ^3\mathrm{He}$ elastic scattering at 450 MeV [38] were used for the outgoing channel. For the incoming channel, the real and imaginary depths of the potentials were scaled by a factor of 0.85 while keeping the other potential parameters the same as those in the outgoing channel, following the procedure described in [39]. Once the $d\sigma/d\Omega(0°)$ was obtained, it was then extrapolated to varnishing Q value ($Q = 0$) to obtain the $(d\sigma/d\Omega)_{q=0}$ by using the following relationship:

$$\left(\frac{d\sigma}{d\Omega}\right)_{q=0} = \left[\frac{\frac{d\sigma}{d\Omega}(Q=0,0°)}{\frac{d\sigma}{d\Omega}(Q,0°)}\right]_{\mathrm{DWBA}} \left[\frac{d\sigma}{d\Omega}(Q,0°)\right]_{\mathrm{exp}}, \quad (2)$$

where the subscripts "DWBA" and "exp" represent the calculated and experimental values, respectively. Following the procedure described above, the $B(\mathrm{GT})$ were determined to be 0.011 ± 0.004 and 0.008 ± 0.003 for the 473- and 571-keV states, respectively. The errors were estimated from the uncertainties in beam intensity (10%), target thickness (15%), tensor-force-induced proportionality breaking (14% for the 473-keV and 24% for the 571-keV states) [17], and statistical fluctuations (20% for the 473-keV and 25% for the 571-keV states).

Impacts on the ^{60}Fe *synthesis in massive stars.*—The stellar β-decay rate of ^{59}Fe was calculated by using the following equation:

$$\lambda = \sum_i \frac{(2J_i+1)e^{-E_i/kT}}{G(T)}\lambda_i, \quad (3)$$

where i represents the ith level in ^{59}Fe. J_i, E_i, and λ_i are the spin, excitation energy, and β-decay rate of the level, respectively. k is the Boltzmann constant and T is temperature. $G(T) = \sum_l (2J_l+1)\exp[-E_l/(kT)]$ is the partition function of ^{59}Fe. Only those transitions indicated in Fig. 1 were considered in Eq. (3) since they dominate the total β-decay rate of ^{59}Fe in the relevant stellar environment. For the ground state, λ_i was derived from the terrestrial half-life of ^{59}Fe. For the 473- and 571-keV excited states, the λ_i was determined by the following equation:

$$\lambda_i = \frac{\ln 2}{K}\left(\frac{g_A}{g_V}\right)^2 B_i \Phi_i, \quad (4)$$

where $K = 6146$ s, $(g_A/g_V)^2 = 1.2599^2$ [40] and Φ_i is the phase space integral. B_i is the $B(\mathrm{GT})$ of the corresponding transition, which was deduced from the present measurement by using the detailed balance theorem.

Figure 3(a) shows the calculated β-decay rate of ^{59}Fe as a function of temperature based on the present measurement and existing theoretical calculations. At low temperatures (e.g., $T = 0.4$ GK during He-shell burning), the decay rates are dominated by the ground state and different calculations shown in Fig. 3(a) gave similar results. With increasing temperature, the decay rates increase rapidly and results from the different calculations start to diverge due to the increasing contribution from the excited states. At temperatures above 0.5 GK, the FFN table overestimates the decay rates, while the LMP one underestimates the rates, with larger discrepancies at higher temperatures. The shell model calculation [12] using the GXPF1j interaction predicted $B(\mathrm{GT})$ values of 0.0074 and 0.0006 for the 473- and 571-keV states, respectively, based on which the calculated decay rate lies closest to our experimentally determined one. At $T = 1.2$ GK, a typical temperature for

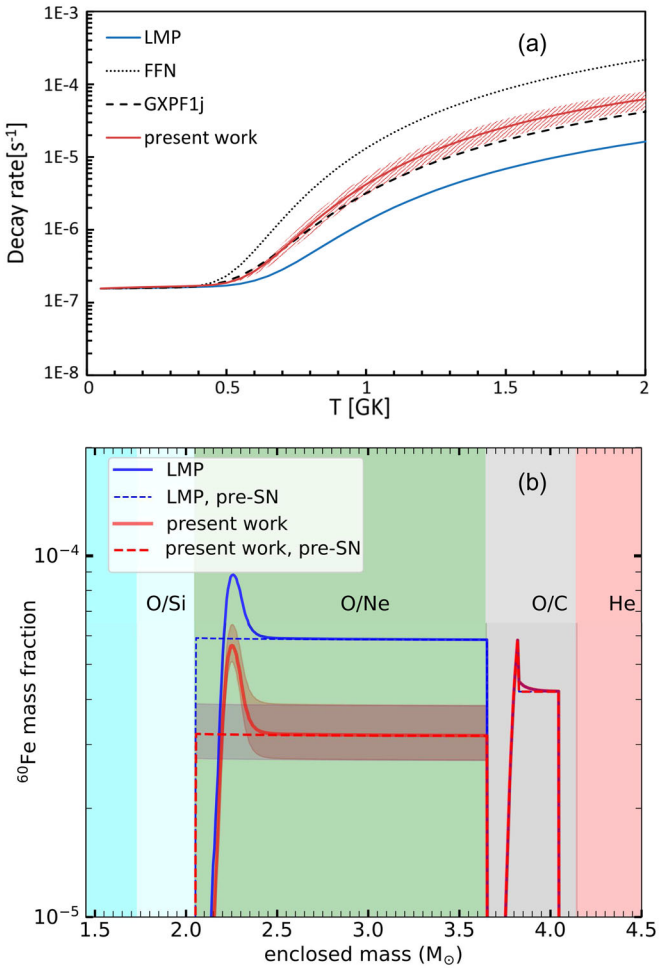

FIG. 3. (a) The stellar β-decay rate of ^{59}Fe as a function of temperature from calculations by LMP (blue solid line) [14], FFN (dotted line) [13], shell model calculation [12] using GXPF1j interaction (dashed line) and the present Letter (red solid line). The shaded area represents the error propagated from the measured $B(\mathrm{GT})$. (b) Calculated ^{60}Fe mass fraction profile by using β-decay rates of ^{59}Fe from LMP and the present Letter. Dashed lines represent the profile before explosion. The shaded background colors indicate different compositional shells defined by the dominant nuclear species at core collapse.

C-shell burning, the β-decay rates are dominated by excited states and are about 2 orders of magnitude larger than that of the ground state. At this temperature, the ^{59}Fe-decay rate based on our measurement is a factor of 3.5 ± 1.1 larger than that from the LMP table, which is currently used most widely in astrophysical simulations.

In order to illustrate the impact of the determined transition strengths in the astrophysical context, we have used the stellar hydrodynamics code KEPLER [41–43] to model the evolution and explosion of a massive star with an initial mass of 18 $M_\odot$ and solar metallicity. The explosion was parametrized by a piston positioned at 1.47 $M_\odot$, where the electron fraction Y_e drops below 0.49. The velocity of the piston was adjusted to lead to an explosion energy of

10^{51} erg. The setup and included physics are mostly the same as in Sukhbold *et al.* [11] and Müller *et al.* [44], but using the solar composition from Lodders *et al.* [45]. We performed the calculation with ^{59}Fe-decay rates based on the central, upper, and lower values of the transition strengths reported here, as well as with the rate from the LMP table.

The result is shown in Fig. 3(b) where the ^{60}Fe mass fraction is plotted as a function of the enclosed mass. Before explosion (pre-SN), two regions of significant ^{60}Fe production can be identified: first, in the O/C shell between 3.7 $M_\odot$ and 4.1 $M_\odot$, ^{60}Fe is synthesized during the He-shell burning. The temperature here is never high enough to affect the ^{59}Fe-decay rate and thus it is not affected by the improved decay rate. Second, between 2 $M_\odot$ and 3.6 $M_\odot$, in the O/Ne shell, ^{60}Fe is produced during convective C-shell burning. Here, the temperature exceeds 1 GK and the thermal population of excited states significantly affects the lifetime of ^{59}Fe. Figure 3(b) shows that the pre-SN ^{60}Fe mass fraction with the central value of the decay rate from our measurement is 3.1×10^{-5}, which is almost half of the value of 5.8×10^{-5} obtained using the rate from the LMP table.

In addition to the pre-SN mass fraction, the solid lines in Figure 3(b) also show the distribution after the explosion. Below the enclosed mass of 2.1 $M_\odot$, where the temperature of the supernova (SN) shock exceeds 3 GK, ^{60}Fe is destroyed, mostly by (n,γ) and (p,n) reactions. At a mass coordinate of 2.2 $M_\odot$, the temperature is just right for additional neutrons provided by ^{22}Ne(α,γ) to lead to another burst of production of ^{60}Fe that is added to the existing pre-SN content. In spite of the high temperature, the ^{59}Fe-decay rate does not affect the explosive component, because the timescales of the explosion are too short for noticeable decay to occur. At larger radii, there is no significant change of the ^{60}Fe mass fraction and the pre-SN component in the O/C shell also remains mostly unaffected by the explosion. With the LMP decay rate, the total ^{60}Fe of this model is 1.02×10^{-4} $M_\odot$, while we find a total yield of $6.20^{+1.01}_{-0.69} \times 10^{-5}$ $M_\odot$ with the experimentally determined transition strengths, corresponding to a decrease of 40%. The new result points to reduced tension in the discrepancy of the ^{60}Fe/^{26}Al γ-ray flux ratio.

It should be noted that the impact of the decay rate depends on the relative contributions of the C- and He-shell burning, as well as on the explosion energy. To investigate the impacts on the Galactic ^{60}Fe in greater detail, more systematic calculations for a range of stellar models need to be carried out, which is beyond the scope of the present Letter. However, our measurement eliminates one of the most important nuclear uncertainties and provides accurate nuclear inputs for future astrophysical simulations.

Summary.—The discrepancy between the observed ^{60}Fe/^{26}Al γ-ray flux ratio and theoretical predictions remains an open question. We have performed, for the first time, exclusive measurement of the important Gamow-Teller strengths from the low-lying states in ^{59}Fe to the ^{59}Co ground state via the ^{59}Co$(t,{}^3$He$)^{59}$Fe charge-exchange reaction. The calculated β-decay rate of ^{59}Fe based on the present measurement is a factor of 3.5 ± 1.1 larger than the currently adopted rate during carbon-shell burning at 1.2 GK. Stellar evolution calculations with an 18 $M_\odot$ star demonstrate the impacts of the new decay rate on the synthesis of ^{60}Fe. A decrease of 40% was found for the yield of ^{60}Fe from our calculation by using the new rate compared to that by using the currently adopted one. More systematic astrophysical calculations are needed to fully investigate the impact on the galactic ^{60}Fe. Our measurement eliminates one of the major uncertainties due to nuclear physics in predicting the yield of ^{60}Fe and alleviates the existing discrepancy of the ^{60}Fe/^{26}Al ratio for some models. This is an important step toward the understanding the ^{60}Fe/^{26}Al ratio.

We thank the NSCL staff for their support during the preparations for and conducting of the experiment. This project is supported by the National Key Research and Development program (MOST 2016YFA0400501). Part of the work was supported by the Strategic Priority Research Program of Chinese Academy of Sciences, Grant No. XDB XDB34020000. GRETINA was funded by the U.S. Department of Energy, in the Office of Nuclear Physics of the Office of Science. Operation of the array at N. S. C. L. was supported by DOE under Awards No. DE-SC0019034 (NSCL) and No. DE-AC02-05CH11231 (LBNL). Part of the work was supported by the U.S.-NSF under Grants No. PHY-1811855 and by the U.S. Department of Energy, Office of Science, Office of Nuclear Physics, under Award No. DE-SC0020451 (MSU). A. S. was supported in part by the U.S. Department of Energy [DE-FG02-87ER40328 (UM)]. Some calculations were performed at the Minnesota Supercomputing Institute.

*gaobsh@impcas.ac.cn
†lika@impcas.ac.cn

[1] F. X. Timmes, S. E. Woosley, D. H. Hartmann, R. D. Hoffman, T. A. Weaver, and F. Matteucci, Astrophys. J. **449**, 204 (1995).
[2] M. Limongi and A. Chieffi, Astrophys. J. **647**, 483 (2006).
[3] S. E. Woosley and A. Heger, Phys. Rep. **442**, 269 (2007), the Hans Bethe Centennial Volume 1906–2006.
[4] A. I. Karakas and J. C. Lattanzio, Pub. Astron. Soc. Aust. **20**, 279 (2003).
[5] M. Lugaro, U. Ott, and Á. Kereszturi, Prog. Part. Nucl. Phys. **102**, 1 (2018).
[6] S. Wanajo, H.-T. Janka, and B. Müller, Astrophys. J. **774**, L6 (2013).
[7] K. Nomoto and S.-C. Leung, Space Sci. Rev. **214**, 67 (2018).
[8] W. Wang, T. Siegert, Z. G. Dai, R. Diehl, J. Greiner, A. Heger, M. Krause, M. Lang, M. M. M. Pleintinger, and X. L. Zhang, Astrophys. J. **889**, 169 (2020).
[9] N. Prantzos, Astron. Astrophys. **420**, 1033 (2004).

[10] A. Chieffi and M. Limongi, Astrophys. J. **764**, 21 (2013).
[11] T. Sukhbold, T. Ertl, S. E. Woosley, J. M. Brown, and H. T. Janka, Astrophys. J. **821**, 38 (2016).
[12] K. A. Li, Y. H. Lam, C. Qi, X. D. Tang, and N. T. Zhang, Phys. Rev. C **94**, 065807 (2016).
[13] G. M. Fuller, W. A. Fowler, and M. J. Newman, Astrophys. J. **252**, 715 (1982).
[14] K. Langanke and G. Martínez-Pinedo, At. Data Nucl. Data Tables **79**, 1 (2001).
[15] M. Honma, T. Otsuka, T. Mizusaki, M. Hjorth-Jensen, and B. A. Brown, J. Phys. **20**, 7 (2005).
[16] R. G. T. Zegers *et al.*, Phys. Rev. Lett. **99**, 202501 (2007).
[17] R. G. T. Zegers *et al.*, Phys. Rev. C **74**, 024309 (2006).
[18] W. P. Alford, B. A. Brown, S. Burzynski, A. Celler, D. Frekers, R. Helmer, R. Henderson, K. P. Jackson, K. Lee, A. Rahav, A. Trudel, and M. C. Vetterli, Phys. Rev. C **48**, 2818 (1993).
[19] D. J. Morrissey, B. M. Sherrill, M. Steiner, A. Stolz, and I. Wiedenhoever, Nucl. Instrum. Methods Phys. Res., Sect. B **204**, 90 (2003), 14th International Conference on Electromagnetic Isotope Separators and Techniques Related to Their Applications.
[20] D. Bazin, J. A. Caggiano, B. M. Sherrill, J. Yurkon, and A. Zeller, Nucl. Instrum. Methods Phys. Res., Sect. B **204**, 629 (2003), 14th International Conference on Electromagnetic Isotope Separators and Techniques Related to Their Applications.
[21] G. Perdikakis, R. G. T. Zegers, S. M. Austin, D. Bazin, C. Caesar, J. M. Deaven, A. Gade, D. Galaviz, G. F. Grinyer, C. J. Guess, C. Herlitzius, G. W. Hitt, M. E. Howard, R. Meharchand, S. Noji, H. Sakai, Y. Shimbara, E. E. Smith, and C. Tur, Phys. Rev. C **83**, 054614 (2011).
[22] J. Yurkon, D. Bazin, W. Benenson, D. J. Morrissey, B. M. Sherrill, D. Swan, and R. Swanson, Nucl. Instrum. Methods Phys. Res., Sect. A **422**, 291 (1999).
[23] S. Paschalis *et al.*, Nucl. Instrum. Methods Phys. Res., Sect. A **709**, 44 (2013).
[24] D. Weisshaar *et al.*, Nucl. Instrum. Methods Phys. Res., Sect. A **847**, 187 (2017).
[25] S. Noji *et al.*, Phys. Rev. Lett. **112**, 252501 (2014).
[26] S. Noji *et al.*, Phys. Rev. C **92**, 024312 (2015).
[27] J. C. Zamora *et al.*, Phys. Rev. C **100**, 032801(R) (2019).
[28] B. Gao *et al.*, Phys. Rev. C **101**, 014308 (2020).
[29] R. Titus *et al.*, Phys. Rev. C **100**, 045805 (2019).
[30] K. C. McLean, S. M. Dalgliesh, S. S. Ipson, and G. Brown, Nucl. Phys. **A191**, 417 (1972).
[31] E. K. Warburton, J. W. Olness, A. M. Nathan, J. J. Kolata, and J. B. McGrory, Phys. Rev. C **16**, 1027 (1977).
[32] R. Vennink, J. Kopecky, P. M. Endt, and P. W. M. Glaudemans, Nucl. Phys. **A344**, 421 (1980).
[33] A. N. Deacon, S. J. Freeman, R. V. F. Janssens, M. Honma, M. P. Carpenter, P. Chowdhury, T. Lauritsen, C. J. Lister, D. Seweryniak, J. F. Smith, S. L. Tabor, B. J. Varley, F. R. Xu, and S. Zhu, Phys. Rev. C **76**, 054303 (2007).
[34] J. H. Bjerregaard, P. F. Dahl, O. Hansen, and G. Sidenius, Nucl. Phys. **51**, 641 (1964).
[35] J. Cook and J. Carr, computer program FOLD/DWHI, Florida State University (unpublished); based on F. Petrovich and D. Stanley, Nucl. Phys. **A275**, 487 (1977); modified as described in J. Cook, K. W. Kemper, P. V. Drumm, L. K. Fifield, M. A. C. Hotchkis, T. R. Ophel, and C. L. Woods, Phys. Rev. C **30**, 1538 (1984); R. G. T. Zegers, S. Fracasso, and G. Colò (unpublished).
[36] S. C. Pieper and R. B. Wiringa, Annu. Rev. Nucl. Part. Sci. **51**, 53 (2001).
[37] M. Honma, T. Otsuka, B. A. Brown, and T. Mizusaki, Eur. Phys. J. A **25**, 499 (2005).
[38] T. Yamagata, H. Utsunomiya, M. Tanaka, S. Nakayama, N. Koori, A. Tamii, Y. Fujita, K. Katori, M. Inoue, M. Fujiwara, and H. Ogata, Nucl. Phys. **A589**, 425 (1995).
[39] S. Y. Van Der Werf, S. Brandenburg, P. Grasduk, W. A. Sterrenburg, M. N. Harakeh, M. B. Greenfield, B. A. Brown, and M. Fujiwara, Nucl. Phys. **A496**, 305 (1989).
[40] I. S. Towner and J. C. Hardy, *Symmetries and Fundamental Interactions in Nuclei*, edited by W. C. Haxton and E. M. Henley (World Scientific, Singapore, 1995), p. 183.
[41] T. A. Weaver, G. B. Zimmerman, and S. E. Woosley, Astrophys. J. **225**, 1021 (1978).
[42] S. E. Woosley, A. Heger, and T. A. Weaver, Rev. Mod. Phys. **74**, 1015 (2002).
[43] A. Heger and S. E. Woosley, Astrophys. J. **724**, 341 (2010).
[44] B. Müller, A. Heger, D. Liptai, and J. B. Cameron, Mon. Not. R. Astron. Soc. **460**, 742 (2016).
[45] K. Lodders, H. Palme, and H. P. Gail, edited by J. E. Trümper, Landolt-Bornstein, New Series, VI, 4B, 712 (Springer-Verlag, Berlin, 2009).